

# Improved bounds on the bosonic dark matter with pulsars in the Milky Way

Dicong Liang,<sup>a</sup> Lijing Shao<sup>a,b,1</sup>

<sup>a</sup>Kavli Institute for Astronomy and Astrophysics, Peking University, Beijing 100871, China

<sup>b</sup>National Astronomical Observatories, Chinese Academy of Sciences, Beijing 100012, China

E-mail: [dcliang@pku.edu.cn](mailto:dcliang@pku.edu.cn), [lshao@pku.edu.cn](mailto:lshao@pku.edu.cn)

**Abstract.** Neutron stars (NSs) can be used to constrain dark matter (DM) since a NS can transform into a black hole (BH) if it captures sufficient DM particles and exceeds the Chandrasekhar limit. We extend earlier work and for the first time take into account the Galactic motion of individual NSs, which changes the amount of the captured DM by as large as one to two orders of magnitude. We systematically apply the analysis to 413 NSs in the Milky Way, and constrain the DM particle mass and its interaction with nucleon simultaneously. We find that the most stringent bound is placed by a few NSs and the bound becomes stronger after considering the Galactic motion. The survival of observed NSs already excludes a cross section  $\sigma_{nX} \gtrsim 10^{-45} \text{ cm}^2$  for DM particles with mass from 100 MeV to  $10^3 \text{ GeV}$ . Especially for a mass around 10 GeV, the constraint on the cross section is as stringent as  $\sigma_{nX} \lesssim 10^{-49} \text{ cm}^2$ .

**Keywords:** dark matter, neutron star, Galactic motion, cross section

---

<sup>1</sup>Corresponding author.

---

## Contents

<b>1</b>	<b>Introduction</b>	<b>1</b>
<b>2</b>	<b>Dark Matter Capture</b>	<b>2</b>
<b>3</b>	<b>Black Hole Formation</b>	<b>5</b>
3.1	Thermalization	5
3.2	Collapse	7
3.3	Growth	7
<b>4</b>	<b>Results and Discussions</b>	<b>8</b>

---

## 1 Introduction

According to contemporary observations, there is a large number of invisible matter, which constitutes about 26% of the total energy of our Universe [1]. This kind of matter does not interact with the electromagnetic field, but manifests itself by the gravitational effect, thus it is called dark matter (DM) [2, 3]. Weakly-interacting massive particle (WIMP), with mass in the range from GeV to TeV, is one of the best motivated candidates of DM [4, 5]. In 1980s, the possible capture of WIMPs by the Sun and the Earth was studied. If WIMPs annihilate inside the Sun or the Earth, it would produce jets of neutrinos that might be detected by neutrino detectors [6–9]. Later, the effects of DM particle annihilation and kinetic heating inside neutron stars (NSs) were discussed [10–22]. After being captured in a NS, DM can change the inner structure of the star [23–37] and leave imprint on gravitational waves [38–51].

If the captured DM concentrates in a very dense region, it can even form a minuscular black hole (BH) inside the NS [52, 53]. Then the small BH can consume the star and finally produce a BH with mass around 1 to 2 solar masses [54–57]. Such a scenario happens only when the NS accretes a large amount of DM, which depends on the interaction cross section between the DM particles and the nucleons [58]. Recently, more progress was made in improving the model of DM capture [59–66]. After being captured, the DM particles lose energy and then thermalize with the NS via repeatedly scattering with nucleons [67, 68]. For asymmetric DM which does not self-annihilate [69, 70], it accumulates in the core of the NS after thermalization, eventually reaches the Chandrasekhar limit, and collapses into a BH [71–73]. The nascent BH grows when its accretion outstrips its Hawking radiation evaporation [74–77], and finally destroys the NS.

If DM particles are bosons, they can form a Bose-Einstein condensate (BEC), and the self-gravity starts for a smaller number of particles, making the gravitational collapse easier to happen [78]. Including the relativistic effects of the NS’s gravitational field on the BEC transition, the bounds on the cross section can be further strengthened [79]. If DM particles are fermions, the gravitational collapse happens

only when the gravity overcomes the Fermi degeneracy pressure. Taking into account Yukawa-type attractive interactions, the number of DM particles necessary for collapse significantly decreases [80]. While it is argued in Refs. [81, 82] that after considering the relativistic effects, the Chandrasekhar limit does not significantly change. Besides, DM self-annihilation and co-annihilation with nucleons can release the bounds on DM [83–85]. A detailed study for both bosonic and fermionic DM can be found in Ref. [86]. Constraining DM via black hole formation in non-compact objects can be found in Ref. [87].

The DM capture rate by a NS depends on the local DM density. As the DM halo density profile is not uniform, the constraint discussed above is dependent on the position of NSs [88]. In literature, NSs were all assumed as static in the Milky Way. But in reality, they are moving around the center of the Galaxy, and some of them can have a large orbital eccentricity, with PSR J1909–3744 being an example (cf. Fig. 11 in Ref. [89]). Therefore, some of these NSs have passed the inner Galactic region during the motion, where the DM density is much higher than their current location. In this paper, we for the first time consider how the Galactic motion of the NSs affects their accretion of DM and then affects the derived bound on the DM-nucleon cross section. We use the GalPot package<sup>1</sup> [90] to calculate the orbits of the NSs, based on the mass model of the Milky Way [91–93]. We find that after taking into account the Galactic motion, the amount of captured DM varies. For some cases, the change is as large as one to two orders of magnitude, compared to their corresponding static cases. In this work we use bosonic DM to illustrate, and the analysis will be applied to fermionic DM in the future.

The paper is organized as follows. In Sec. 2, we calculate the orbits of NSs in the Milky Way and compare the amount of captured DM with the static cases. Then, we discuss details about the mechanism for DM to form a BH inside the NS in Sec. 3. Finally, we use a catalog of NSs to place improved constraint on the DM, and discuss the results in Sec. 4.

## 2 Dark Matter Capture

We assume that NSs have mass  $M_{\text{NS}} \simeq 1.5 M_{\odot}$ , radius  $R_{\text{NS}} \simeq 11$  km, inner temperature  $T_{\text{NS}} \simeq 10^6$  K, and a uniform density  $\rho_B = M_{\text{NS}} / (\frac{4}{3}\pi R_{\text{NS}}^3)$ . The escape velocity at the surface of a NS is  $v_{\text{esc}} = \sqrt{2GM_{\text{NS}}/R_{\text{NS}}}$ . We denote  $m_X$  the mass of DM particle, and  $\sigma_{nX}$  the cross section of the interaction between DM particle and neutron. We consider that the velocity of DM particles follows the Maxwell-Boltzmann distribution, and the velocity dispersion is  $\bar{v}_X$ .

A DM particle is captured when it loses enough energy after scattering with nucleon. Taking relativistic effects into account, the capture rate is given by [72, 84, 88],

$$C_{X,0} = \sqrt{\frac{6}{\pi}} \left( \frac{\rho_{\text{DM}}}{\bar{v}_X} \right) \frac{\xi N_B v_{\text{esc}}^2}{m_X} \left[ 1 - \frac{1 - \exp(-B^2)}{B^2} \right] f(\sigma_{nX}). \quad (2.1)$$

---

<sup>1</sup><https://github.com/PaulMcMillan-Astro/GalPot/tree/master>

Here  $N_B$  is the total number of neutrons within the star,  $m_B$  is the mass of the neutron,  $\rho_{\text{DM}}$  is the density of DM. The factor

$$B^2 = \frac{v_{\text{esc}}^2}{\bar{v}_X^2} \frac{6m_X m_B}{(m_X - m_B)^2}, \quad (2.2)$$

accounts for the minimum energy loss necessary to capture the DM [72], and the parameter  $\xi = \min\{\sqrt{2}m_r v_{\text{esc}}/p_F, 1\} \simeq \min\{m_X/(0.2 \text{ GeV}), 1\}$  accounts for the suppression in the capture rate due to the Pauli blocking [72, 85, 88]. Here,  $m_r$  is the dark matter-neutron reduced mass and  $p_F$  is the Fermi momentum. The function  $f(\sigma_{nX}) = \sigma_{\text{sat}}[1 - e^{-\sigma_{nX}/\sigma_{\text{sat}}}]$  with  $\sigma_{\text{sat}} = R_{\text{NS}}^2/(0.45N_B\xi)$  gives the probability that a DM particle scatters [84].

In literature, NSs are treated as static, but in fact their Galactic motion cannot be neglected during their whole lifetime. When we consider the Galactic motion of NSs,  $\rho_{\text{DM}}$  is no longer constant for each NS but varies with time, that is,  $\rho_{\text{DM}} = \rho_{\text{DM}}(\mathbf{r}(t))$ . To reconstruct the Galactic motion of NSs, we make use of the data in the Australia Telescope National Facility (ATNF) pulsar catalogue<sup>2</sup> [94] to set up the initial conditions, i.e. the position and velocity of the stars. For most of the NSs, the proper motion in right ascension and declination, namely, the transverse velocity can be derived from timing observations. While the radial velocity  $v_r$  is difficult to measure, thus, it remains unknown for most of the NSs. We select 413 NSs from the ATNF catalogue, whose sky location, proper motion and distance are known. Then, we consider three configurations where we assume  $v_r = 0, -100 \text{ km/s},$  and  $100 \text{ km/s},$  respectively, so that we have the full three-dimension velocity. With the Galactic gravitational potential provided by McMillan [93] and the position and velocity of the stars, we use GalPot package [90] to integrate the Galactic motion of these NSs backward in time for the duration of their characteristic age,  $t_{\text{NS}}$ . The parameter  $t_{\text{NS}}$  in the ATNF catalog is estimated by the spin-down of the star [94], and it might be overestimated, especially for the millisecond pulsars that have undergone the *recycling* processes [95]. Thus, for those NSs whose characteristic age  $t_{\text{NS}} > 10 \text{ Gyr}$ , we set their age to be  $t_{\text{NS}} = 10 \text{ Gyr}$ .

Galactic motions are calculated for all the selected 413 NSs. Taking three NSs, PSRs J1909–3744, J1959+2048 and J0453+1559 as examples, we show their Galactic motion in Fig. 1. To make the trajectory more clear, we only show the motion in the past 500 Myr. Following Liu et al. [89], the coordinate system is chosen such that the origin is the Galactic center and the X-Y plane coinciding with the Galactic plane. For PSR J1909–3744, the shape of the orbit does not change much with respect to different radial velocity,  $v_r$ . While for PSR J1959+2048, the orbits are significantly different from each other when  $v_r$  is different. PSR J0453+1559 is an example of small orbital eccentricity.

When calculating the orbit, we have made use of the best fitting Galactic potential model of the Milky Way [93], in which the DM density distribution is modeled by the

---

<sup>2</sup><https://www.atnf.csiro.au/people/pulsar/psrcat/>

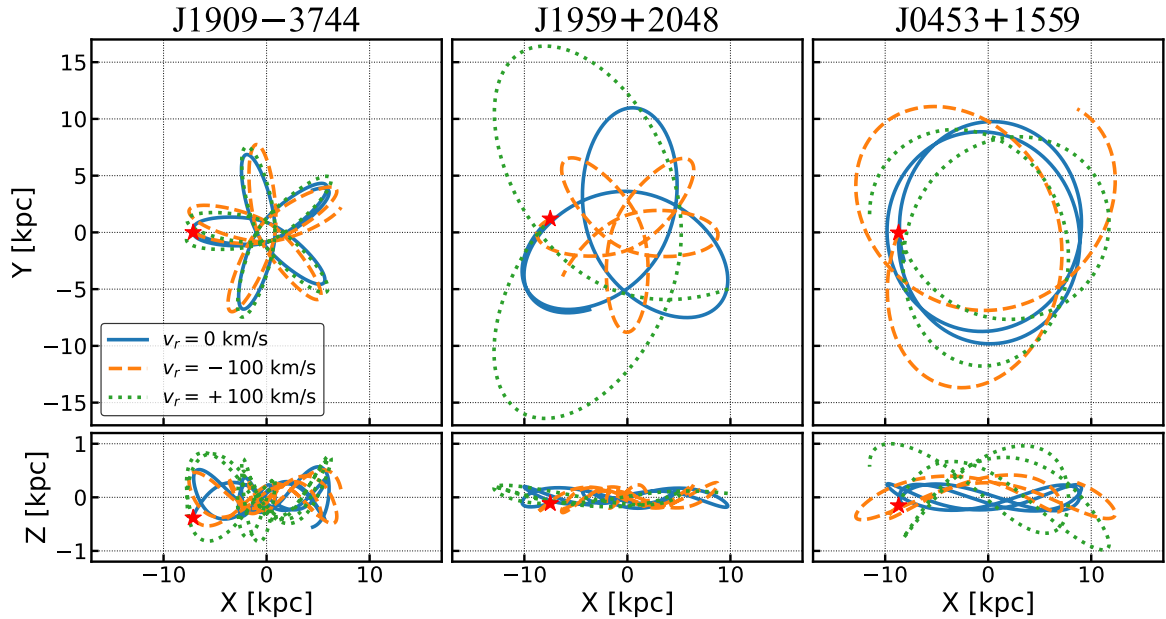


**Figure 1.** Galactic motion of three pulsars in the past 500 Myr. The red star denotes the current position of the pulsars.

Navarro-Frenk-White profile [96] ,

$$\rho_{\text{DM}}(r) = \frac{\rho_{0,h}}{(r/r_h)^\gamma (1 + 3r/r_h)^{3-\gamma}}, \quad (2.3)$$

where  $\gamma = 1$ , and  $r_h = 18.6$  kpc is the scale radius. The parameter  $\rho_{0,h}$  is a normalized factor such that the local DM density, namely the density at the Solar system, is  $\rho_{\text{DM}}(r = 8.20 \text{ kpc}) = 0.38 \text{ GeV/cm}^3$ .

In addition, when we take into account the relative motion between the NS and the DM halo, there is correction factor  $\zeta$  on the capture rate, as was indicated in Refs. [8, 61]:

$$C_X = \zeta C_{X,0}, \quad (2.4)$$

where

$$\zeta = \left[ 1 - \frac{1 - \exp(-B^2)}{B^2} \right]^{-1} \left\{ \frac{(B_+ B_- - 1/2)[\chi(-\eta, \eta) - \chi(B_-, B_+)]}{2\eta B^2} + \frac{B_+ \exp(-B_-^2)/2 - B_- \exp(-B_+^2)/2 - \eta \exp(-\eta^2)}{2\eta B^2} \right\}, \quad (2.5)$$

$\chi(a, b) \equiv \int_a^b \exp(-y^2) dy = \sqrt{\pi}[\text{erf}(b) - \text{erf}(a)]/2$ ,  $B_\pm \equiv B \pm \eta$  and  $\eta = \sqrt{3/2} v_\star / \bar{v}_X$ . Here,  $v_\star$  is the relative velocity between the NS and the DM halo. When  $\eta \rightarrow 0$ , i.e. the NS is static relative to the DM halo, then  $\zeta \rightarrow 1$ . In addition, we have

$$\zeta \rightarrow \zeta_\infty \equiv \frac{\sqrt{\pi} \text{erf}(\eta)}{2\eta}, \quad (2.6)$$

when  $B \gg 1$ . At the same time, we also consider that the velocity dispersion of DM  $\bar{v}_X$  varies with different radius from the Galactic center. Here we adopt the so-called standard halo model and assume the velocity dispersion is isotropic, then we have [97–99]

$$\bar{v}_X = \sqrt{3/2}v_c, \quad (2.7)$$

where  $v_c = v_c(r(t))$  is the circular velocity at the radius  $r$  from the Galactic center. Notice that, we get  $v_*$  and  $v_c$  from the GalPot package. For the Milky Way model [93] we consider in this paper, we have  $v_c \lesssim 233$  km/s. For  $m_X$  in the range from  $10^{-3}$  GeV to  $10^3$  GeV, we have  $B \gtrsim 50$ , then  $\zeta$  can be approximated as  $\zeta_\infty$ , which only depends on  $\eta$ . For most of the NSs, we have  $\eta \lesssim 2$ , then  $\zeta \gtrsim 0.44$ . For  $m_X \ll 10^{-3}$  GeV or  $m_X \gg 10^3$  GeV, then we have  $B \rightarrow 0$  thus  $\zeta \rightarrow \exp(-\eta^2)$ , the suppression of the capture is even more significant.

To compare the amount of DM captured with and without the consideration of Galactic motion, we introduce a parameter, the capture ratio  $R_c$ , which estimates the ratio between the moving case and the corresponding static case. The capture ratio is defined as,

$$R_c := \frac{N_X^{(m)}}{N_X^{(s)}} = \frac{\int_0^{t_{\text{NS}}} dt C_X(t)}{\int_0^{t_{\text{NS}}} dt C_{X,0}} = \frac{\bar{A}}{A_0} \equiv \frac{\frac{1}{t_{\text{NS}}} \int_0^{t_{\text{NS}}} dt \rho_{\text{DM}}(t)\zeta(t)\bar{v}_{X,s}/\bar{v}_X(t)}{\rho_{\text{DM},0}\bar{v}_{X,s}/\bar{v}_{X,0}}. \quad (2.8)$$

Here,  $N_X$  is the total number of DM particles captured by the NS, and the superscripts “(m)” and “(s)” stand for the moving case and static case respectively. In the denominator, the NS is assumed to be static, which means we used the current location of the NS to calculate  $\rho_{\text{DM},0}$  and  $\bar{v}_{X,0}$ . Here, we introduce a typical velocity  $\bar{v}_{X,s} = 200$  km/s to make  $\bar{A}$  and  $A_0$  have the same dimension as  $\rho_{\text{DM}}$ .

Based on their Galactic motion, we calculated the capture ratio for 413 NSs, and the results are shown in Fig. 2. As we can see, the largest ratio is larger than 3 while the smallest ratio is about 0.003. Thus, after considering the Galactic motion, the capture amount of DM can change by about one to two orders of magnitude, compared to the static cases. For most of the NSs, the capture is suppressed due to the relative motion between the NSs and the DM halo. While for some of the NSs,  $R_c > 1$  since they have moved inwards to denser DM region where  $\bar{v}_X$  is smaller and  $\rho_{\text{DM}}$  is much larger, so that the effect outstrips the suppression  $\zeta$ .

### 3 Black Hole Formation

In this section, we consider three physical processes after the DM particles are captured by the NS, namely, thermalization, collapse, and growth. These three stages are important for the DM to eventually engulf the NS.

#### 3.1 Thermalization

After being captured, the DM particles lose energy via repeated scattering with nucleons and then attain thermal equilibrium with the star. Ignoring nuclear interactions and approximating the neutrons as a dense, non-interacting Fermi gas, the

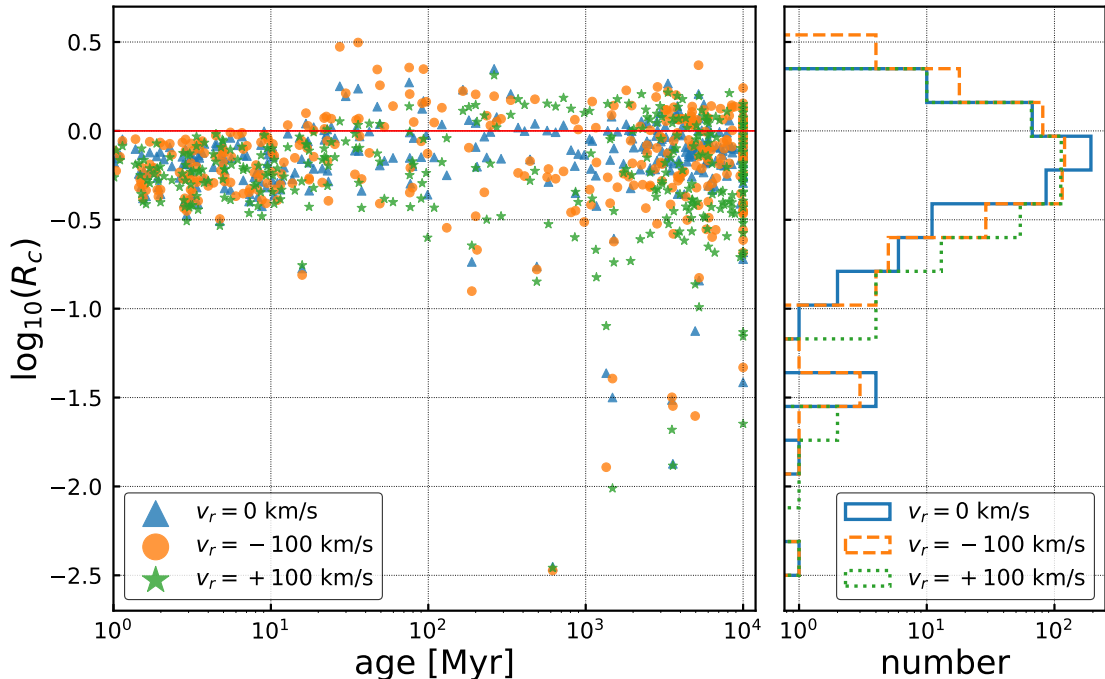


**Figure 2.** Distribution of the logarithm of the capture ratio  $R_c$ . On the left panel, we show the distribution of  $\log_{10}(R_c)$  and the age of 413 NSs. We use different markers to denote three cases where the radial velocity  $v_r = 0, -100, +100$  km/s. On the right panel, we show the histograms of the numbers.

timescale of thermalization can be estimated as [67],

$$t_{\text{th}} = \frac{105\pi^2\hbar^3}{16k_b^2T_{\text{NS}}^2m_B\sigma_{nX}} \frac{m_X/m_B}{(1+m_X/m_B)^2} = 75 \text{ yr} \left( \frac{10^{-45} \text{ cm}^2}{\sigma_{nX}} \right) \frac{m_X/m_B}{(1+m_X/m_B)^2}. \quad (3.1)$$

Here,  $k_b$  is the Boltzmann constant. To form a BH inside NS, we need that the thermalization finishes within the lifetime of the NS, i.e.,

$$t_{\text{th}} < t_{\text{NS}}. \quad (3.2)$$

We call Eq. (3.2) the ‘‘Condition Thermalization.’’ As the DM thermalizes, it accumulates within a sphere of radius  $r_{\text{th}}$ , which is

$$r_{\text{th}} = \sqrt{\frac{9k_bT_{\text{NS}}}{8\pi G\rho_B m_X}} = 8.8 \text{ m} \left( \frac{\text{GeV}}{m_X} \right)^{1/2}, \quad (3.3)$$

where we have used the virial theorem

$$\frac{GM_B(r_{\text{th}})m_X}{r_{\text{th}}} = \frac{3}{2}k_bT_{\text{NS}}. \quad (3.4)$$

We consider that the DM particles collect inside the NS, specifically, we require the thermalization radius  $r_{\text{th}} \lesssim 0.2R_{\text{NS}}$  [85], which gives a constraint that

$$m_X \gtrsim 1.6 \times 10^{-5} \text{ GeV}. \quad (3.5)$$



### 3.2 Collapse

To collapse into a BH, the accumulated DM has to form a self-gravitating system. For bosonic DM, after it concentrates at the core of the NS, it can undergo a phase transition to a BEC state, which has a higher density than a thermal gas-like state. Then the self-gravitation starts at a critical particle number

$$N_X > N_{\text{BEC}}. \quad (3.6)$$

For a Newtonian potential, McDermott et al. [72] provided the derivation of  $N_{\text{BEC}}$ , while for a compact object like NS, it is necessary to consider the relativistic effects. After deriving an effective gravitational potential energy, Jamison [79] gave the critical number for BEC, that is

$$N_{\text{BEC}} = \zeta(3) \left( \frac{k_B T_{\text{NS}}}{\hbar \sqrt{4\pi G(\rho_B + 3P_B)/3}} \right)^3 = 5.6 \times 10^{38} \left( \frac{T_{\text{NS}}}{10^6 \text{ K}} \right)^3. \quad (3.7)$$

Here, we have adopted  $P_B = 0.3\rho_B$  as in Ref. [100]. Since  $N_{\text{BEC}} \propto T_{\text{NS}}^3$ , the critical number for BEC reduces significantly for a cooler NS.

If we do not consider self-interaction, the critical number for Chandrasekhar limit is  $N_{\text{Cha}} = 2m_{\text{pl}}^2/(\pi m_X^2)$ , where  $m_{\text{pl}}$  is the Planck mass [101]. When we consider a bosonic field with a self-coupling term  $\lambda|\phi|^4$ , the Chandrasekhar limit becomes larger [102],

$$N_{\text{Cha}} = \frac{2m_{\text{pl}}^2}{\pi m_X^2} \left( 1 + \frac{\lambda m_{\text{pl}}^2}{32\pi m_X^2} \right)^{1/2}. \quad (3.8)$$

Such a repulsive self-interaction becomes stronger when  $\lambda$  is larger. In this paper, we adopt  $\lambda = 10^{-30}$  as in Refs. [83, 88]. The DM will collapse when

$$N_X - N_{\text{BEC}} > N_{\text{Cha}}. \quad (3.9)$$

We call Eq. (3.9) as the ‘‘Condition Collapse.’’ Notice that  $N_{\text{Cha}}$  monotonically decreases when  $m_X$  increases, and we have

$$N_{\text{Cha}} \simeq \begin{cases} 1.2 \times 10^{41} \left( \frac{\text{GeV}}{m_X} \right)^3, & m_X \ll 10^3 \text{ GeV}, \\ 9.5 \times 10^{37} \left( \frac{\text{GeV}}{m_X} \right)^2, & m_X \gg 10^3 \text{ GeV}. \end{cases} \quad (3.10)$$

For  $T_{\text{NS}} = 10^6 \text{ K}$ , we have  $N_{\text{Cha}} = N_{\text{BEC}}$  when  $m_X = 5.9 \text{ GeV}$ . Thus, the Condition Collapse becomes  $N_X \gtrsim N_{\text{Cha}}$  for  $m_X \ll 5.9 \text{ GeV}$ , and  $N_X \gtrsim N_{\text{BEC}}$  for  $m_X \gg 5.9 \text{ GeV}$ .

### 3.3 Growth

After its formation in the interior of the NS, the BH accretes the ordinary matter inside the NS, which can be described by the Bondi accretion [103],

$$\left( \frac{dM_{\text{BH}}}{dt} \right)_{\text{Bondi}} = \frac{4\pi\lambda_s\rho_B(GM_{\text{BH}})^2}{v_s^3}. \quad (3.11)$$



Here,  $M_{\text{BH}} = N_{\text{Cha}} m_X$  is the mass of BH when it forms. The parameter  $\lambda_s = 0.25$  is the accretion eigenvalue for the transonic solution, and  $v_s$  is the sound speed in the NS, which we approximate to be  $0.17c$  as in Ref. [85]. At the same time, the BH also dissipates via Hawking radiation. Thus, the BH will grow only when the following condition satisfies,

$$\frac{4\pi\lambda_s\rho_B(GM_{\text{BH}})^2}{v_s^3} - \frac{\hbar c^4}{15360\pi(GM_{\text{BH}})^2} + C_X m_X > 0, \quad (3.12)$$

where the second term corresponds to Hawking radiation. The third term corresponds to the accretion of the dark matter, since all newly captured particles go to the ground state directly after a BEC is formed [72, 73, 86]. In other words, when the accretion of both the ordinary matter and the dark matter exceeds the Hawking radiation, the BH will grow. The continuous growth of the BH will eventually destroy the NS. Here we call Eq. (3.12) as the ‘‘Condition Growth.’’

## 4 Results and Discussions

If the Conditions Thermalization, Collapse and Growth, i.e., Eqs. (3.2), (3.9) and (3.12), are satisfied simultaneously, the DM will form a BH inside the NS and then engulf the star. Thus, we can use the current observational fact that these NSs exist to exclude the parameter space where all these three conditions are met.

As we can see in Fig. 1, PSR J1959+2048 has quite different motion for different choices of  $v_r$ . For this NS, we have  $R_c = 0.80, 1.39,$  and  $0.35,$  for  $v_r = 0, -100$  km/s, and  $+100$  km/s, respectively. Thus, here we take it as an example in Fig. 3, to illustrate the constraints in different scenarios. For the static case, we use brown lines with different styles to denote different conditions; the excluded parameter space is shaded in light brown. We also show the boundary of the excluded parameter space in other three moving cases with dot-dot-dashed lines in different colors.

Now, we analyze the constraint in details. Considering Eqs. (2.1) and (2.4), we have  $1 \geq 1 - (1 - e^{-B^2})/B^2 \geq 0.8$  for the mass range from  $10^{-6}$  GeV to  $10^6$  GeV, thus we approximate this factor to be 1 for the following estimation. If  $\sigma_{nX} \ll \sigma_{\text{sat}}$ , we have

$$N_X \approx 2.1 \times 10^{42} \left( \frac{\bar{A}}{\text{GeV}/\text{cm}^3} \right) \left( \frac{t_{\text{NS}}}{\text{Gyr}} \right) \left( \frac{\text{GeV}}{m_X} \right) \frac{\sigma_{nX}}{\sigma_{\text{sat}}}. \quad (4.1)$$

For  $5.9 \text{ GeV} > m_X > 0.2 \text{ GeV}$ , the Condition Collapse, namely  $N_X \gtrsim N_{\text{Cha}}$ , gives the bound on the cross section,

$$\sigma_{nX} \gtrsim 8.2 \times 10^{-47} \text{ cm}^2 \left( \frac{\text{GeV}/\text{cm}^3}{\bar{A}} \right) \left( \frac{\text{Gyr}}{t_{\text{NS}}} \right) \left( \frac{\text{GeV}}{m_X} \right)^2. \quad (4.2)$$

For PSR J1959+2048, it just corresponds to the left boundary of the constraint curve (brown dashed line) in Fig. 3, whose slope is  $k \simeq -2$  in the logarithm scale. While for  $m_X > 5.9 \text{ GeV}$ , the Condition Collapse, namely  $N_X \gtrsim N_{\text{BEC}}$ , gives the bound,

$$\sigma_{nX} \gtrsim 4.0 \times 10^{-47} \text{ cm}^2 \left( \frac{\text{GeV}/\text{cm}^3}{\bar{A}} \right) \left( \frac{\text{Gyr}}{t_{\text{NS}}} \right) \left( \frac{m_X}{100 \text{ GeV}} \right). \quad (4.3)$$

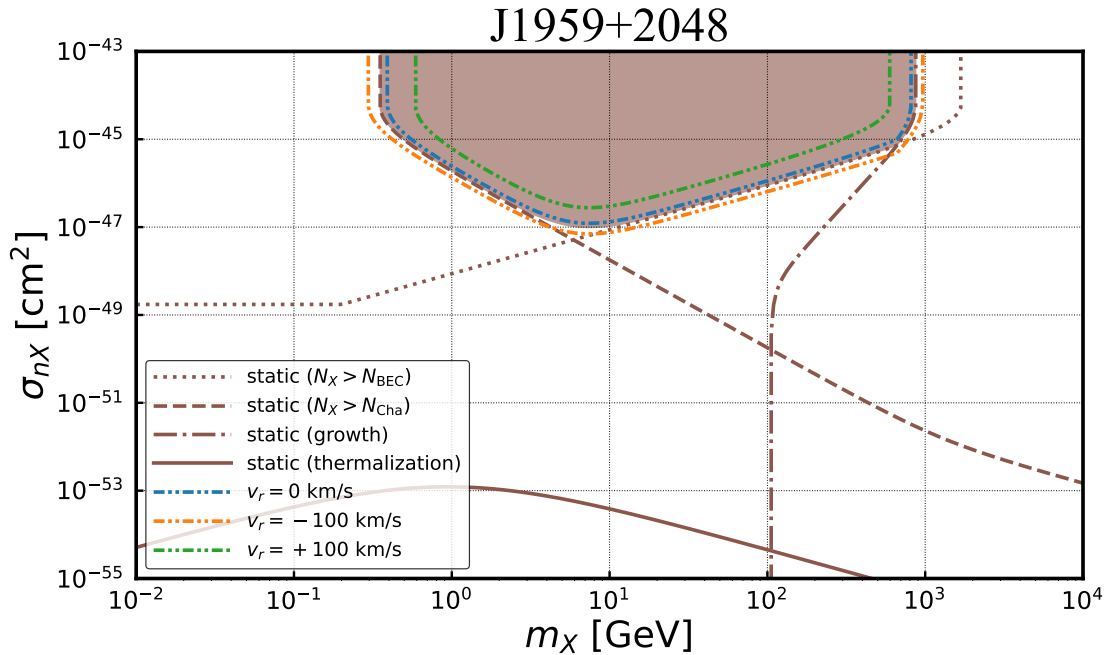


**Figure 3.** Constraint on the DM-nucleon cross section  $\sigma_{nX}$  from PSR J1959+2048. We use dotted, dashed, dot-dashed and solid lines in brown to denote Eqs. (3.6), (3.8), (3.12) and (3.2), respectively. The shaded brown area represents the excluded parameter space due to the simultaneous satisfaction of the three conditions, that will deconstruct the NS. The blue, orange, and green dot-dot-dashed lines correspond to the constraint in the cases where  $v_r = 0, -100$  km/s, and  $+100$  km/s, respectively.

It corresponds to the right boundary (brown dotted line) in Fig. 3, whose slope is  $k \simeq 1$ . When  $\sigma_{nX} \gg \sigma_{\text{sat}}$ , we have  $1 - \exp(-\sigma_{nX}/\sigma_{\text{sat}}) \rightarrow 1$ . For the lower mass range, we have  $N_{\text{Cha}} > N_{\text{BEC}}$ , thus  $N_X \gtrsim N_{\text{Cha}}$  gives the lower cutoff of the mass of the DM particle,

$$m_X \gtrsim 2.3 \times 10^{-1} \text{ GeV} \left( \frac{\text{GeV}/\text{cm}^3}{\bar{A}} \right)^{1/2} \left( \frac{\text{Gyr}}{t_{\text{NS}}} \right)^{1/2}, \quad (4.4)$$

while  $N_X \gtrsim N_{\text{BEC}}$  gives the higher cutoff,

$$m_X \lesssim 3.8 \times 10^3 \text{ GeV} \left( \frac{\bar{A}}{\text{GeV}/\text{cm}^3} \right) \left( \frac{t_{\text{NS}}}{\text{Gyr}} \right). \quad (4.5)$$

For most NSs that are old enough, the Condition Thermalization is satisfied trivially. Now we discuss the Condition Growth. Considering only the first two terms in Eq. (3.12), we get a conservative condition for the growth of BH,

$$M_{\text{BH}} \geq \left( \frac{\hbar c^4 v_s^3}{61440 \pi^2 G^4 \lambda_s \rho_B} \right)^{1/4} = 9.1 \times 10^{36} \text{ GeV}, \quad (4.6)$$

which corresponds to

$$m_X \leq 113 \text{ GeV}. \quad (4.7)$$

It means that for  $m_X \leq 113 \text{ GeV}$ , the BH always grows after formation, which is the lower cutoff for the dot-dashed brown curve in Fig. 3. While Eq. (3.12) gives the higher cutoff, which is  $m_X \lesssim 931 \text{ GeV} [\bar{A}/(\text{GeV}/\text{cm}^3)]^{1/2}$  for  $\bar{A} \gg 7 \text{ GeV}/\text{cm}^3$  and  $m_X \lesssim 1064 \text{ GeV} [\bar{A}/(\text{GeV}/\text{cm}^3)]^{1/4}$  for  $\bar{A} \ll 7 \text{ GeV}/\text{cm}^3$ . The boundary for  $\sigma_{nX}$  is

$$\sigma_{nX} \gtrsim 1.9 \times 10^{-48} \text{ cm}^2 \left( \frac{m_X}{200 \text{ GeV}} \right)^4 \left( \frac{\text{GeV}/\text{cm}^3}{\bar{A}} \right), \quad (4.8)$$

when  $m_X < 1000 \text{ GeV}$ , thus the slope is  $k \simeq 4$  (brown dot-dashed line) in Fig. 3.

From above analysis, we find that the boundary from Condition Collapse relies on  $\bar{A}$  and  $t_{\text{NS}}$ , and the boundary from Condition Growth only depends on  $\bar{A}$ . Thus, the survival of those old NSs in the center of Milky Way where the DM density is high, will give the most stringent constraint. Now, We use all the data from the 413 NSs to place a combined constraint, and the results are shown in Fig. 4. For each NS, there is a thin grey line, representing the boundary of the excluded parameter space. For the parameter space above the boundary, a BH will form and destroy the star. Thus, the outer envelope of these lines represents for the combined constraint. As we can see in Fig. 4, the most stringent constraint comes from a few NSs, such as PSR J1801–3210. These few NSs are highlighted with thick dashed lines.

To compare the moving cases with the static cases, we calculate the ratio between the outer envelop of the combined constraint curve, namely,

$$R_\sigma = \frac{\sigma_{nX}^{(m)}}{\sigma_{nX}^{(s)}}. \quad (4.9)$$

As we can see in Eqs. (4.2), (4.3) and (4.8), the boundary  $\sigma_{nX} \propto 1/\bar{A}$ , thus we have

$$R_\sigma \simeq \frac{A_0}{\bar{A}} = \frac{1}{R_c}, \quad (4.10)$$

for the same  $m_X$ . Since the boundary is primarily determined by PSR J1801–3210, we take it as an example. We find that  $R_\sigma = 0.81, 0.91,$  and  $0.92$  for  $v_r = 0, -100 \text{ km/s},$  and  $+100 \text{ km/s},$  respectively. The ratio  $R_\sigma < 1$  means that we can exclude the smaller cross section for the moving cases compared to the static case. Notice that, the value of  $\bar{A}$  varies case by case for the four highlighted NSs. It is majorly due to the different orbits in the past, and is influenced by the radial velocity, as shown in Fig. 1. When we measure the radial velocity of pulsars in the future, we can construct more realistic orbits.

To conclude, for the first time we consider how the Galactic motion of NSs affects their accretion of DM. With the motion of the NSs, the DM density and velocity dispersion changes with time. The relative motion between the NSs and the DM halo suppresses the capture efficiency. For some of the NSs, the capture amount can change by as large as one to two orders of magnitude, compared to the static cases. We use the survival of NSs to constrain the mass of the DM particle and the cross section. The envelope of constraints from 413 NSs gives an improved bound. In the future, we need

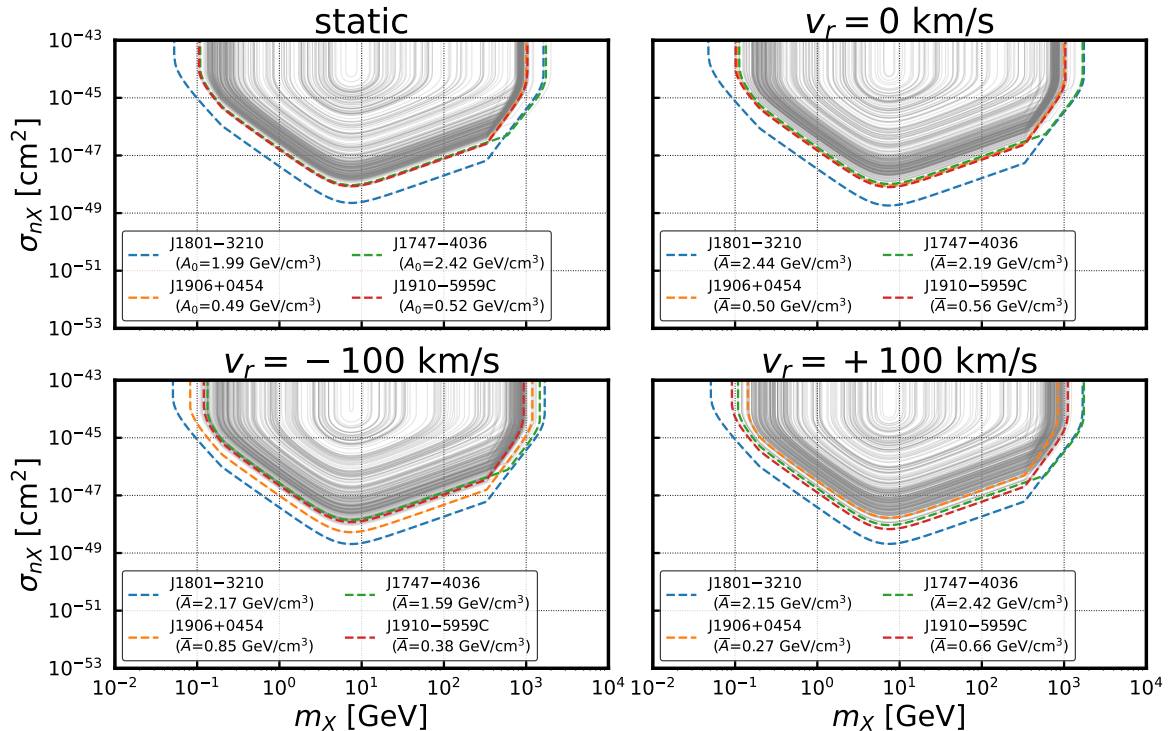


**Figure 4.** Constraints from 413 NSs. Each NS gives a thin grey line, and the parameter space above that line is excluded due to the survival of that NS. Overall, a few NSs contribute to the most outer bound, and these NSs are denoted as thick dashed lines.

more precise measurement of the radial velocity to construct the precise trajectory of NSs. The age of NSs also needs to be determined properly to place more realistic constraints. The effects of the age of NSs on the constraint on the cross section can be estimated by Eqs. (4.2) and (4.3). In this work, we have only considered bosonic DM particles, but a similar analysis can be applied to the fermionic DM, which we leave to a future work. Last but not least, we treat the NSs as density-uniform object and adopt the escape velocity at the surface of the star to simplify the calculation, as in Refs. [72, 84, 88]. While, in reality, the inner structure of NS is much more complicated, which also affects the capture of DM, as was indicated in Ref. [61]. It will be another interesting topic in the future to discuss how different equation of states of NS affect the capture of NS.

## Acknowledgments

We acknowledge the referee for the useful comments which help us improve the manuscript. We thank Zexin Hu, Xueli Miao, Zhongpeng Sun, Yichen Wang and Norbert Wex for helpful discussion. This work was supported by the China Postdoctoral Science Foundation (2021TQ0018), the National SKA Program of China (2020SKA0120300), the National Natural Science Foundation of China (11975027,

11991053), the Max Planck Partner Group Program funded by the Max Planck Society, and the High-Performance Computing Platform of Peking University.

## References

- [1] PLANCK collaboration, *Planck 2018 results. VI. Cosmological parameters*, *Astron. Astrophys.* **641** (2020) A6 [[1807.06209](#)].
- [2] G. Bertone, D. Hooper and J. Silk, *Particle dark matter: Evidence, candidates and constraints*, *Phys. Rept.* **405** (2005) 279 [[hep-ph/0404175](#)].
- [3] D. Clowe, M. Bradac, A. H. Gonzalez, M. Markevitch, S. W. Randall, C. Jones et al., *A direct empirical proof of the existence of dark matter*, *Astrophys. J. Lett.* **648** (2006) L109 [[astro-ph/0608407](#)].
- [4] G. Jungman, M. Kamionkowski and K. Griest, *Supersymmetric dark matter*, *Phys. Rept.* **267** (1996) 195 [[hep-ph/9506380](#)].
- [5] J. L. Feng, *Dark Matter Candidates from Particle Physics and Methods of Detection*, *Ann. Rev. Astron. Astrophys.* **48** (2010) 495 [[1003.0904](#)].
- [6] W. H. Press and D. N. Spergel, *Capture by the sun of a galactic population of weakly interacting massive particles*, *Astrophys. J.* **296** (1985) 679.
- [7] A. Gould, *WIMP Distribution in and Evaporation From the Sun*, *Astrophys. J.* **321** (1987) 560.
- [8] A. Gould, *Resonant Enhancements in WIMP Capture by the Earth*, *Astrophys. J.* **321** (1987) 571.
- [9] A. Gould, *Direct and Indirect Capture of Wimps by the Earth*, *Astrophys. J.* **328** (1988) 919.
- [10] C. Kouvaris, *WIMP Annihilation and Cooling of Neutron Stars*, *Phys. Rev. D* **77** (2008) 023006 [[0708.2362](#)].
- [11] G. Bertone and M. Fairbairn, *Compact Stars as Dark Matter Probes*, *Phys. Rev. D* **77** (2008) 043515 [[0709.1485](#)].
- [12] C. Kouvaris and P. Tinyakov, *Can Neutron stars constrain Dark Matter?*, *Phys. Rev. D* **82** (2010) 063531 [[1004.0586](#)].
- [13] M. McCullough and M. Fairbairn, *Capture of Inelastic Dark Matter in White Dwarves*, *Phys. Rev. D* **81** (2010) 083520 [[1001.2737](#)].
- [14] J. Bramante, A. Delgado and A. Martin, *Multiscatter stellar capture of dark matter*, *Phys. Rev. D* **96** (2017) 063002 [[1703.04043](#)].
- [15] M. Baryakhtar, J. Bramante, S. W. Li, T. Linden and N. Raj, *Dark Kinetic Heating of Neutron Stars and An Infrared Window On WIMPs, SIMPs, and Pure Higgsinos*, *Phys. Rev. Lett.* **119** (2017) 131801 [[1704.01577](#)].
- [16] N. Raj, P. Tanedo and H.-B. Yu, *Neutron stars at the dark matter direct detection frontier*, *Phys. Rev. D* **97** (2018) 043006 [[1707.09442](#)].
- [17] N. F. Bell, G. Busoni and S. Robles, *Heating up Neutron Stars with Inelastic Dark Matter*, *JCAP* **09** (2018) 018 [[1807.02840](#)].

- [18] D. A. Camargo, F. S. Queiroz and R. Sturani, *Detecting Dark Matter with Neutron Star Spectroscopy*, *JCAP* **09** (2019) 051 [[1901.05474](#)].
- [19] J. F. Acevedo, J. Bramante, R. K. Leane and N. Raj, *Warming Nuclear Pasta with Dark Matter: Kinetic and Annihilation Heating of Neutron Star Crusts*, *JCAP* **03** (2020) 038 [[1911.06334](#)].
- [20] T. N. Maity and F. S. Queiroz, *Detecting bosonic dark matter with neutron stars*, *Phys. Rev. D* **104** (2021) 083019 [[2104.02700](#)].
- [21] T. T. Q. Nguyen and T. M. P. Tait, *Bounds on Long-lived Dark Matter Mediators from Neutron Stars*, [2212.12547](#).
- [22] S. Chatterjee, R. Garani, R. K. Jain, B. Kanodia, M. S. N. Kumar and S. K. Vempati, *Faint light of old neutron stars from dark matter capture and detectability at the James Webb Space Telescope*, [2205.05048](#).
- [23] F. Sandin and P. Ciarcelluti, *Effects of mirror dark matter on neutron stars*, *Astropart. Phys.* **32** (2009) 278 [[0809.2942](#)].
- [24] M. A. Perez-Garcia, J. Silk and J. R. Stone, *Dark matter, neutron stars and strange quark matter*, *Phys. Rev. Lett.* **105** (2010) 141101 [[1007.1421](#)].
- [25] S. C. Leung, M. C. Chu and L. M. Lin, *Equilibrium Structure and Radial Oscillations of Dark Matter Admixed Neutron Stars*, *Phys. Rev. D* **85** (2012) 103528 [[1205.1909](#)].
- [26] X. Li, F. Wang and K. S. Cheng, *Gravitational effects of condensate dark matter on compact stellar objects*, *JCAP* **10** (2012) 031 [[1210.1748](#)].
- [27] M. A. Perez-Garcia, F. Daigne and J. Silk, *Short GRBs and dark matter seeding in neutron stars*, *Astrophys. J.* **768** (2013) 145 [[1303.2697](#)].
- [28] I. Goldman, R. N. Mohapatra, S. Nussinov, D. Rosenbaum and V. Teplitz, *Possible Implications of Asymmetric Fermionic Dark Matter for Neutron Stars*, *Phys. Lett. B* **725** (2013) 200 [[1305.6908](#)].
- [29] Q.-F. Xiang, W.-Z. Jiang, D.-R. Zhang and R.-Y. Yang, *Effects of fermionic dark matter on properties of neutron stars*, *Phys. Rev. C* **89** (2014) 025803 [[1305.7354](#)].
- [30] Z. Rezaei, *Study of Dark-Matter Admixed Neutron Stars using the Equation of State from the Rotational Curves of Galaxies*, *Astrophys. J.* **835** (2017) 33 [[1612.02804](#)].
- [31] S. Mukhopadhyay, D. Atta, K. Imam, D. N. Basu and C. Samanta, *Compact bifluid hybrid stars: Hadronic Matter mixed with self-interacting fermionic Asymmetric Dark Matter*, *Eur. Phys. J. C* **77** (2017) 440 [[1612.07093](#)].
- [32] J. Ellis, G. Hütsi, K. Kannike, L. Marzola, M. Raidal and V. Vaskonen, *Dark Matter Effects On Neutron Star Properties*, *Phys. Rev. D* **97** (2018) 123007 [[1804.01418](#)].
- [33] H. C. Das, A. Kumar, B. Kumar, S. Kumar Biswal, T. Nakatsukasa, A. Li et al., *Effects of dark matter on the nuclear and neutron star matter*, *Mon. Not. Roy. Astron. Soc.* **495** (2020) 4893 [[2002.00594](#)].
- [34] H. C. Das, A. Kumar, B. Kumar, S. K. Biswal and S. K. Patra, *Impacts of dark matter on the curvature of the neutron star*, *JCAP* **01** (2021) 007 [[2007.05382](#)].
- [35] B. Kain, *Dark matter admixed neutron stars*, *Phys. Rev. D* **103** (2021) 043009 [[2102.08257](#)].



- [36] T. Gleason, B. Brown and B. Kain, *Dynamical evolution of dark matter admixed neutron stars*, *Phys. Rev. D* **105** (2022) 023010 [2201.02274].
- [37] S. Shakeri and D. R. Karkevandi, *Bosonic Dark Matter in Light of the NICER Precise Mass-Radius Measurements*, 2210.17308.
- [38] J. Ellis, A. Hektor, G. Hütsi, K. Kannike, L. Marzola, M. Raidal et al., *Search for Dark Matter Effects on Gravitational Signals from Neutron Star Mergers*, *Phys. Lett. B* **781** (2018) 607 [1710.05540].
- [39] A. Nelson, S. Reddy and D. Zhou, *Dark halos around neutron stars and gravitational waves*, *JCAP* **07** (2019) 012 [1803.03266].
- [40] J. Kopp, R. Laha, T. Opferkuch and W. Shepherd, *Cuckoo's eggs in neutron stars: can LIGO hear chirps from the dark sector?*, *JHEP* **11** (2018) 096 [1807.02527].
- [41] A. Das, T. Malik and A. C. Nayak, *Confronting nuclear equation of state in the presence of dark matter using GW170817 observation in relativistic mean field theory approach*, *Phys. Rev. D* **99** (2019) 043016 [1807.10013].
- [42] S. Alexander, E. McDonough, R. Sims and N. Yunes, *Hidden-Sector Modifications to Gravitational Waves From Binary Inspirals*, *Class. Quant. Grav.* **35** (2018) 235012 [1808.05286].
- [43] A. Quddus, G. Panotopoulos, B. Kumar, S. Ahmad and S. K. Patra, *GW170817 constraints on the properties of a neutron star in the presence of WIMP dark matter*, *J. Phys. G* **47** (2020) 095202 [1902.00929].
- [44] C. J. Horowitz and S. Reddy, *Gravitational Waves from Compact Dark Objects in Neutron Stars*, *Phys. Rev. Lett.* **122** (2019) 071102 [1902.04597].
- [45] H. C. Das, A. Kumar and S. K. Patra, *Effects of dark matter on the in-spiral properties of the binary neutron stars*, *Mon. Not. Roy. Astron. Soc.* **507** (2021) 4053 [2104.01815].
- [46] H. C. Das, A. Kumar and S. K. Patra, *Dark matter admixed neutron star as a possible compact component in the GW190814 merger event*, *Phys. Rev. D* **104** (2021) 063028 [2109.01853].
- [47] M. Bezares, D. Viganò and C. Palenzuela, *Gravitational wave signatures of dark matter cores in binary neutron star mergers by using numerical simulations*, *Phys. Rev. D* **100** (2019) 044049 [1905.08551].
- [48] A. Das, T. Malik and A. C. Nayak, *Dark matter admixed neutron star properties in light of gravitational wave observations: A two fluid approach*, *Phys. Rev. D* **105** (2022) 123034 [2011.01318].
- [49] Y. Dengler, J. Schaffner-Bielich and L. Tolos, *Second Love number of dark compact planets and neutron stars with dark matter*, *Phys. Rev. D* **105** (2022) 043013 [2111.06197].
- [50] M. Collier, D. Croon and R. K. Leane, *Tidal Love numbers of novel and admixed celestial objects*, *Phys. Rev. D* **106** (2022) 123027 [2205.15337].
- [51] D. R. Karkevandi, S. Shakeri, V. Sagun and O. Ivanytskyi, *Bosonic dark matter in neutron stars and its effect on gravitational wave signal*, *Phys. Rev. D* **105** (2022) 023001 [2109.03801].



- [52] I. Goldman and S. Nussinov, *Weakly Interacting Massive Particles and Neutron Stars*, *Phys. Rev. D* **40** (1989) 3221.
- [53] A. Gould, B. T. Draine, R. W. Romani and S. Nussinov, *Neutron Stars: Graveyard of Charged Dark Matter*, *Phys. Lett. B* **238** (1990) 337.
- [54] C. Kouvaris, P. Tinyakov and M. H. G. Tytgat, *NonPrimordial Solar Mass Black Holes*, *Phys. Rev. Lett.* **121** (2018) 221102 [[1804.06740](#)].
- [55] B. Dasgupta, R. Laha and A. Ray, *Low Mass Black Holes from Dark Core Collapse*, *Phys. Rev. Lett.* **126** (2021) 141105 [[2009.01825](#)].
- [56] R. Garani, D. Levkov and P. Tinyakov, *Solar mass black holes from neutron stars and bosonic dark matter*, *Phys. Rev. D* **105** (2022) 063019 [[2112.09716](#)].
- [57] S. Bhattacharya, B. Dasgupta, R. Laha and A. Ray, *Can LIGO Detect Asymmetric Dark Matter?*, [2302.07898](#).
- [58] T. Güver, A. E. Erkoca, M. Hall Reno and I. Sarcevic, *On the capture of dark matter by neutron stars*, *JCAP* **05** (2014) 013 [[1201.2400](#)].
- [59] J. Lopes, T. Lacroix and I. Lopes, *Towards a more rigorous treatment of uncertainties on the velocity distribution of dark matter particles for capture in stars*, *JCAP* **01** (2021) 073 [[2007.15927](#)].
- [60] N. F. Bell, G. Busoni, T. F. Motta, S. Robles, A. W. Thomas and M. Virgato, *Nucleon Structure and Strong Interactions in Dark Matter Capture in Neutron Stars*, *Phys. Rev. Lett.* **127** (2021) 111803 [[2012.08918](#)].
- [61] N. F. Bell, G. Busoni, S. Robles and M. Virgato, *Improved Treatment of Dark Matter Capture in Neutron Stars*, *JCAP* **09** (2020) 028 [[2004.14888](#)].
- [62] N. F. Bell, G. Busoni, S. Robles and M. Virgato, *Improved Treatment of Dark Matter Capture in Neutron Stars II: Leptonic Targets*, *JCAP* **03** (2021) 086 [[2010.13257](#)].
- [63] F. Anzuini, N. F. Bell, G. Busoni, T. F. Motta, S. Robles, A. W. Thomas et al., *Improved treatment of dark matter capture in neutron stars III: nucleon and exotic targets*, *JCAP* **11** (2021) 056 [[2108.02525](#)].
- [64] D. Bose and S. Sarkar, *Impact of galactic distributions in celestial capture of dark matter*, [2211.16982](#).
- [65] B. Dasgupta, A. Gupta and A. Ray, *Dark matter capture in celestial objects: Improved treatment of multiple scattering and updated constraints from white dwarfs*, *JCAP* **08** (2019) 018 [[1906.04204](#)].
- [66] B. Dasgupta, A. Gupta and A. Ray, *Dark matter capture in celestial objects: light mediators, self-interactions, and complementarity with direct detection*, *JCAP* **10** (2020) 023 [[2006.10773](#)].
- [67] B. Bertoni, A. E. Nelson and S. Reddy, *Dark Matter Thermalization in Neutron Stars*, *Phys. Rev. D* **88** (2013) 123505 [[1309.1721](#)].
- [68] R. Garani, A. Gupta and N. Raj, *Observing the thermalization of dark matter in neutron stars*, *Phys. Rev. D* **103** (2021) 043019 [[2009.10728](#)].
- [69] K. Petraki and R. R. Volkas, *Review of asymmetric dark matter*, *Int. J. Mod. Phys. A* **28** (2013) 1330028 [[1305.4939](#)].

- [70] K. M. Zurek, *Asymmetric Dark Matter: Theories, Signatures, and Constraints*, *Phys. Rept.* **537** (2014) 91 [1308.0338].
- [71] A. de Lavallaz and M. Fairbairn, *Neutron Stars as Dark Matter Probes*, *Phys. Rev. D* **81** (2010) 123521 [1004.0629].
- [72] S. D. McDermott, H.-B. Yu and K. M. Zurek, *Constraints on Scalar Asymmetric Dark Matter from Black Hole Formation in Neutron Stars*, *Phys. Rev. D* **85** (2012) 023519 [1103.5472].
- [73] C. Kouvaris and P. Tinyakov, *Constraining Asymmetric Dark Matter through observations of compact stars*, *Phys. Rev. D* **83** (2011) 083512 [1012.2039].
- [74] C. Kouvaris and P. Tinyakov, *(Not)-constraining heavy asymmetric bosonic dark matter*, *Phys. Rev. D* **87** (2013) 123537 [1212.4075].
- [75] Y.-z. Fan, R.-z. Yang and J. Chang, *Constraining Asymmetric Bosonic Non-interacting Dark Matter with Neutron Stars*, **1204.2564**.
- [76] C. Kouvaris and P. Tinyakov, *Growth of Black Holes in the interior of Rotating Neutron Stars*, *Phys. Rev. D* **90** (2014) 043512 [1312.3764].
- [77] W. E. East and L. Lehner, *Fate of a neutron star with an endoparasitic black hole and implications for dark matter*, *Phys. Rev. D* **100** (2019) 124026 [1909.07968].
- [78] C. Kouvaris and P. Tinyakov, *Excluding Light Asymmetric Bosonic Dark Matter*, *Phys. Rev. Lett.* **107** (2011) 091301 [1104.0382].
- [79] A. O. Jamison, *Effects of gravitational confinement on bosonic asymmetric dark matter in stars*, *Phys. Rev. D* **88** (2013) 035004 [1304.3773].
- [80] C. Kouvaris, *Limits on Self-Interacting Dark Matter*, *Phys. Rev. Lett.* **108** (2012) 191301 [1111.4364].
- [81] M. I. Gresham and K. M. Zurek, *Asymmetric Dark Stars and Neutron Star Stability*, *Phys. Rev. D* **99** (2019) 083008 [1809.08254].
- [82] R. Garani, M. H. G. Tytgat and J. Vandecasteele, *Condensed dark matter with a Yukawa interaction*, *Phys. Rev. D* **106** (2022) 116003 [2207.06928].
- [83] J. Bramante, K. Fukushima and J. Kumar, *Constraints on bosonic dark matter from observation of old neutron stars*, *Phys. Rev. D* **87** (2013) 055012 [1301.0036].
- [84] J. Bramante, K. Fukushima, J. Kumar and E. Stopnitzky, *Bounds on self-interacting fermion dark matter from observations of old neutron stars*, *Phys. Rev. D* **89** (2014) 015010 [1310.3509].
- [85] N. F. Bell, A. Melatos and K. Petraki, *Realistic neutron star constraints on bosonic asymmetric dark matter*, *Phys. Rev. D* **87** (2013) 123507 [1301.6811].
- [86] R. Garani, Y. Genolini and T. Hambye, *New Analysis of Neutron Star Constraints on Asymmetric Dark Matter*, *JCAP* **05** (2019) 035 [1812.08773].
- [87] A. Ray, *Celestial Objects as Strongly-Interacting Asymmetric Dark Matter Detectors*, **2301.03625**.
- [88] J. Bramante and T. Linden, *Detecting Dark Matter with Imploding Pulsars in the Galactic Center*, *Phys. Rev. Lett.* **113** (2014) 191301 [1405.1031].

- [89] K. Liu et al., *A revisit of PSR J1909–3744 with 15-yr high-precision timing*, *Mon. Not. Roy. Astron. Soc.* **499** (2020) 2276 [[2009.12544](#)].
- [90] P. J. McMillan, “GalPot: Galaxy potential code.” Astrophysics Source Code Library, record ascl:1611.006, Nov., 2016.
- [91] W. Dehnen and J. Binney, *Mass models of the Milky Way*, *Mon. Not. Roy. Astron. Soc.* **294** (1998) 429 [[astro-ph/9612059](#)].
- [92] P. J. McMillan, *Mass models of the Milky Way*, *Mon. Not. Roy. Astron. Soc.* **414** (2011) 2446 [[1102.4340](#)].
- [93] P. J. McMillan, *The mass distribution and gravitational potential of the Milky Way*, *Mon. Not. Roy. Astron. Soc.* **465** (2017) 76 [[1608.00971](#)].
- [94] R. N. Manchester, G. B. Hobbs, A. Teoh and M. Hobbs, *The Australia Telescope National Facility pulsar catalogue*, *Astron. J.* **129** (2005) 1993 [[astro-ph/0412641](#)].
- [95] T. M. Tauris, N. Langer and M. Kramer, *Formation of millisecond pulsars with CO white dwarf companions - II. Accretion, spin-up, true ages and comparison to MSPs with He white dwarf companions*, *Mon. Not. Roy. Astron. Soc.* **426** (2012) 1601 [[1206.1862](#)].
- [96] J. F. Navarro, C. S. Frenk and S. D. White, *A Universal density profile from hierarchical clustering*, *Astrophys. J.* **490** (1997) 493 [[astro-ph/9611107](#)].
- [97] A. M. Green, *Dependence of direct detection signals on the WIMP velocity distribution*, *JCAP* **10** (2010) 034 [[1009.0916](#)].
- [98] R. Catena and P. Ullio, *The local dark matter phase-space density and impact on WIMP direct detection*, *JCAP* **05** (2012) 005 [[1111.3556](#)].
- [99] L. E. Strigari, *Galactic Searches for Dark Matter*, *Phys. Rept.* **531** (2013) 1 [[1211.7090](#)].
- [100] A. W. Steiner, J. M. Lattimer and E. F. Brown, *The Neutron Star Mass-Radius Relation and the Equation of State of Dense Matter*, *Astrophys. J. Lett.* **765** (2013) L5 [[1205.6871](#)].
- [101] R. Ruffini and S. Bonazzola, *Systems of selfgravitating particles in general relativity and the concept of an equation of state*, *Phys. Rev.* **187** (1969) 1767.
- [102] M. Colpi, S. L. Shapiro and I. Wasserman, *Boson Stars: Gravitational Equilibria of Selfinteracting Scalar Fields*, *Phys. Rev. Lett.* **57** (1986) 2485.
- [103] S. L. Shapiro and S. A. Teukolsky, *Black holes, white dwarfs, and neutron stars : the physics of compact objects*. 1983.